

1 **Influence of heating rates on the products of high-temperature pyrolysis of waste wood**
2 **pellets and biomass model compounds**

3
4 **Chidi E. Efika¹, Jude A. Onwudili^{2,*}, Paul T, Williams¹**

5 ¹School of Chemical and Process Engineering, University of Leeds, Leeds, LS2 9 JT, UK

6 ²School of Engineering and Applied Sciences, Aston University, Birmingham, B4 7ET, UK

7
8 **Abstract**

9 The effect of heating rates ranging from 5 °C min⁻¹ to 350 °C min⁻¹ on the yields of pyrolysis
10 products of wood and its main pseudo-components (cellulose, hemicellulose and lignin) have
11 been investigated at a temperature of 800 °C in a horizontal fixed bed reactor. Results showed
12 a successive dramatic increase and decrease in gas and liquid yields, respectively, while the
13 yields of solid products showed a gradual decrease as heating rates increased. Increased gas
14 formation and an increasingly aromatic oil/tar support the theory of rapid devolatilization of
15 degradation products with increasing heating rate, leading to extensive cracking of primary
16 pyrolysis vapours. Solid products with coal-like calorific value and large surface areas were
17 obtained. CO became the dominant gas both on a mass and volume basis, at the heating rate of
18 350 °C min⁻¹ for all samples except xylan, which also produced a significant yield of CO₂ (20.3
19 wt% and 25.4 vol%) compared to the other samples. Cellulose produced a gas product with
20 highest calorific value of 35 MJ kg⁻¹ at the highest heating rate. Results also indicate that the
21 three main pseudo-components of biomass each exert a different influence on the products of
22 high temperature wood pyrolysis.

23 **Keywords:** high-temperature pyrolysis, heating rate, woody biomass, high-CV gas products

24
25 *Corresponding Author

26 Email: j.onwudili@aston.ac.uk (J. A. Onwudili)

27 Telephone: +44(0)121 204 4703

28 **1.0 Introduction**

29 Biomass pyrolysis is one of the most advanced thermochemical technologies for biomass
30 conversion into renewable fuels and chemicals. Pyrolysis of biomass is generally characterized
31 by both primary and secondary reactions (Mayes & Broadbelt, 2012; Mettler et al., 2012;
32 Patwardhan et al., 2011b; Zhang et al., 2014). Primary reactions include mainly solid-phase
33 processes such as drying, dehydration, thermal degradation, crosslinking and devolatilization,
34 (Patwardhan et al., 2011b; Zhang et al., 2014). Secondary reactions involve mainly gas-phase
35 as well as gas-solid reactions such as steam reforming, dry reforming, methanation and
36 hydrogenation, water-gas shift/reverse water-gas shift, polymerization and condensation
37 (Patwardhan et al., 2011a; Patwardhan et al., 2011b). Some named secondary reactions include
38 Boudouard reaction, Diels-Alder reaction, Sabatier reaction, etc. A complex combination of
39 these reactions results in the formation of liquid/tar, gaseous and solid products during biomass
40 pyrolysis.

41

42 The predominant reactions and eventual products' distribution during the pyrolysis process are
43 determined by nature of biomass feedstock and process conditions including the type of reactor.
44 The nature of biomass refers to its type, the thermal and physical properties as well as chemical
45 compositions. In terms of pyrolysis process conditions, important parameters such as reaction
46 temperature, heating rate, reaction pressure, residence times and presence of catalysts (Sun et
47 al., 2010; Wang et al., 2008; Wei et al., 2006; Zanzi et al., 2002) play vital roles in influencing
48 the relative yields and compositions of the pyrolysis products. Heating rate, final temperature
49 and presence of a catalyst may be used to tune the distribution and composition of products.
50 Depending on the reactor configuration, temperature, heating rate and vapour residence times

51 have the greatest influence on the prevailing pyrolysis regime ranging from slow to ultra-fast
52 pyrolysis (Wang et al., 2008). The distribution of pyrolysis products therefore depends on how
53 these three parameters, in addition to feedstock type, are managed. In general for a given
54 feedstock, heating rate and temperature influence the rate of biomass degradation and
55 devolatilization, which influence the chemical properties of the initial pyrolysis intermediate
56 species, from which eventual molecular pyrolysis products are formed. In a fluidised bed
57 reactor, small particle sizes, fast heating rates and short residence times ensure that fast
58 pyrolysis is achieved at different temperatures above 400 °C, leading to a majority liquid
59 product via mainly primary reactions. In a fixed bed reactor, high temperatures and high
60 heating rates can lead to high degradation and devolatilization rates, which may lead to the
61 formation of highly reactive intermediate species (e.g. radicals). Even under short residence
62 times, these devolatilized reactive species could react with each other to give different final
63 pyrolysis products.

64

65 In the literature particular attention is paid to the study of pyrolysis for liquid fuel production
66 leading to a wealth of data on studies of so-called fast and flash pyrolysis processes, where the
67 aim is rapid heating rates and rapid volatile quenching ; and slow pyrolysis (Duman et al.,
68 2011; Elliott, 2013; Lam et al., 2017; Li et al., 2004; Luo et al., 2004; Onay & Kockar, 2003;
69 Patwardhan et al., 2011a; Patwardhan et al., 2011b; Sun et al., 2010). However, pyrolysis is
70 involved in any heat treatment of biomass particles, whether considered as the main step or
71 part of a succession of steps in the process (Blondeau & Jeanmart, 2012), hence studies on high
72 temperature pyrolysis which are also relevant to processes such as gasification and combustion,
73 contribute to the understanding of thermochemical biomass conversion.

74

75 High temperature pyrolysis of biomass, when combined with appropriate heating rates can be
76 used to obtain high yields of high calorific value gas products and tars with consistent chemical
77 compositions (Blondeau & Jeanmart, 2012; Zanzi et al., 1996). In this case, high temperatures
78 would provide the activation energies required to break most covalent bonds in biomass,
79 leading to formation of light molecular weight species. Researchers have reported that higher
80 temperatures promote the production of gaseous process products comprising of hydrogen,
81 methane, CO and CO₂; evidenced by increased gas volumes due to enhanced cracking and
82 devolatilization reactions (Çaglar & Demirbas, 2002; Demirbas, 2002; Dufour et al., 2009;
83 Williams, 2005; Zanzi et al., 2002). High temperature pyrolysis of biomass to obtain increased
84 yields of H₂, CO and CH₄ and reduced CO₂ have been reported (Wei et al., 2006; Zanzi et al.,
85 2002). Hydrogen, CO and CH₄ can be used directly as fuels or for making synthetic
86 hydrocarbon fuels and chemicals. Gas heating values of above 18 MJ Nm⁻³ have been reported
87 for pyrolysis temperatures above 750 °C up to 900 °C (Fagbemi et al., 2001). Biomass
88 conversions to gas of up to 87 wt% for temperatures above 800 °C to 1000 °C have been
89 reported (Dupont et al., 2008). Concentrations of H₂ of above 28 mol% and combined H₂ and
90 CO of above 65 mol% (Li et al., 2004) and 70 - 80 vol% (Sun et al., 2010) have been reported
91 for the pyrolysis of biomass at high temperatures (800 °C) without catalysts resulting in an
92 increased H₂/CO ratio. However, high temperature also favours the cracking of tar (Zanzi et
93 al., 2002) to hydrocarbon gases like CH₄ and C₂H₄, which tend to decompose into carbon
94 (char) and H₂ when the temperature is high enough (Dufour et al., 2009; Guoxin et al., 2009;
95 Kantarelis et al., 2009; Sun et al., 2010). In addition, the same factors that favour increased
96 pyrolysis gas formation may inadvertently lead to simplification of components of oil/tar
97 products into organic compounds with simple structures, which are often useful. Therefore,
98 further cracking and condensation of hydrocarbon gases can lead to the production of simple
99 but highly stable aromatic hydrocarbons (Kantarelis et al., 2009). Furthermore, increased

100 volatile yields have been reported (Beis et al., 2002; Meesri & Moghtaderi, 2002; Seebauer et
101 al., 1997) at high heating rates compared to lower heating rate pyrolysis at the same
102 temperature. This resulted from enhanced process severity impacted by rapid formation and
103 evolution of small volatile molecules during pyrolysis. Such rapid volatile mass losses due to
104 high heating rates could leave behind a solid residue with tuneable pore structure (Cetin et al.,
105 2005; Zanzi et al., 1996), which may be advantageous for further applications e.g. as catalyst
106 supports, water treatment or tar cracking.

107

108 In this present study, a lignocellulosic biomass sample in the form of waste wood pellets and
109 the three main biochemical components of biomass (lignin, cellulose and hemicellulose) have
110 been separately subjected to high temperature pyrolysis under different heating rates. A
111 detailed analysis of the reaction products may shed some light on whether the three components
112 interact during biomass pyrolysis. This will contribute to the understanding of the effects of
113 temperature and heating rates on yields and composition of products from biomass and its
114 components under the pyrolysis conditions used in this work. The novelty of this study is to
115 provide experimental data as a basis for evaluating and applying this type of pyrolysis process
116 as a biomass pre-processing technology for subsequent biomass valorisation into liquid fuels
117 and chemicals. The main focus of this work will be on the gaseous and liquid products, which
118 are useful for liquid fuels and chemicals production.

119

120 **2.0 Materials and Methods**

121

122 **2.1 Materials**

123 Waste wood pellets with dimensions of 6 mm diameter and 14 mm length, were originally
124 made from pinewood sawdust. For this study, the wood pellets were ground and sieved to ≈ 1

125 mm particle size. The biomass components in the form of cellulose (microcrystalline), lignin
126 (Kraft alkali) and hemicellulose (xylan) samples used were each of particle size $< 180 \mu\text{m}$. The
127 cellulose was supplied by Avocado Research Chemicals, UK, while lignin and hemicellulose
128 samples were obtained from Sigma-Aldrich, UK. These were used as is without further
129 treatment. The proximate and ultimate compositions of the samples were determined using a
130 Stanton-Redcroft Thermogravimetric analyser (TGA) and a Carlo Erba Flash EA 112
131 elemental analyser, respectively. The results of these analyses are presented in Table 1. The
132 moisture contents of the samples determined by TGA analysis were 6.4, 4.7, 4.1 and 6.7 wt%
133 for wood, cellulose, lignin and xylan respectively.

134

135 Pyrolysis experiments were carried out in a purpose-built horizontal fixed bed reactor, shown
136 in Figure 1. The reactor was made up of a horizontal stainless steel cylindrical tube of length
137 650 mm and internal diameter of 11 mm. The reactor was heated externally by a Carbolite
138 electrical tube furnace which provides a heated zone of length 450 mm and can be easily
139 controlled to provide the desired final temperature and heating rate. The sample was introduced
140 to the reactor via a sample boat, which was a stainless steel cylindrical tube with a cup at its
141 end for holding the sample. The sample boat was designed to be easily, horizontally inserted
142 into and withdrawn from one end of the reactor. During experiments, the sample boat was
143 placed at the centre of the reactor's heated zone for effective heating. A thermocouple was also
144 integrated into the sample boat, designed to be placed concentric to the walls of the sample
145 boat, thereby providing the temperature at the centre of the sample.

146

147 **2.2 Procedure for pyrolysis**

148 Experiments involving the effect of heating rates ($5, 90$ and $350 \text{ }^\circ\text{C min}^{-1}$) were performed to
149 a final temperature of $800 \text{ }^\circ\text{C}$. All experiments were performed with 1.0 g of the each sample

150 loaded unto the sample boat and inserted into the reactor which was continually swept with
151 inert nitrogen gas at a flow rate of 100 mL min⁻¹. The pyrolysis vapour residence time within
152 the reactor was estimated as 9 seconds based on the reactor volume and nitrogen flow rate. The
153 actual sample heating rates were monitored with the thermocouple inserted at the centre of the
154 sample boat and these were found to be very close to the reactor heating rate. Pyrolysis vapours
155 were purged from the reactor by the nitrogen flow into two sets of glass condensers; the first
156 was water-cooled and the second with a glass wool trap was immersed in dry ice. The non-
157 condensable gases were collected in a sampling bag for off-line analysis by gas
158 chromatography (GC). Solid products remained in the sample boat and were weighed and
159 collected for analysis after the reactor cooled. Each experiment was carried out twice in order
160 to determine repeatability and the reliability of the pyrolysis reactor, under identical conditions.
161 Experimental results were reproducible within 3.5%, indicating that the reactor used in this
162 work was reliable for pyrolysis investigations.

163

164 **2.3 Analysis of pyrolysis products**

165 **2.3.1. Gas Analysis**

166 Non-condensable gases which were collected in the sample gas bag were analysed by GC. A
167 Varian 3380GC with dual packed columns and dual thermal conductivity detectors (GC/TCD)
168 was used to analyse and determine the yields of permanent gases (H₂, CO, O₂, N₂ and CO₂).
169 The column for CO₂ analysis was of 2 m length by 2 mm diameter with Haysep 80 – 100 mesh
170 packing material. Analysis for H₂, CO, O₂ and N₂ was carried out in a second column of 2 m
171 length by 2 mm diameter packed with 60 – 80 mesh molecular sieve. A second Varian 3380
172 GC with a flame ionization detector (GC/FID) was used to analyse and determine the yields of
173 hydrocarbons gases (CH₄, C₂H₄, C₂H₆, C₃H₆, C₃H₈, C₄H₈ and C₄H₁₀) with nitrogen carrier gas.
174 The column was 2 m length by 2mm diameter, packed with Haysep 80 – 100 mesh. The

175 conditions used for the analysis have been detailed elsewhere (Efika et al., 2015). The higher
176 heating value (HHV) of the gas products were calculated from the Equation 1 below;

177

178 $HHV = CV_m / Z_m$ (1)

179

180 Where CV_m is the sum of the products of the weight percent and the calorific values of the
181 individual gases and Z_m is the compressibility factor of the gases.

182 **2.3.2 Oil/Tar Analysis**

183 Due to the high temperatures > 700 °C used in this work, the condensable volatiles would be
184 referred to as a mixture of oil and tar. The condensed products collected in the condensers for
185 each experiment were weighed and then sampled for qualitative analysis by gas
186 chromatography/mass spectrometry (GC/MS) and Fourier transforms infra-red (FTIR). The
187 product collected in the first condenser was brownish in colour and sticky while that collected
188 in the second condenser was a mixture of water and a pale yellow liquid. The products from
189 the two condensers were sampled with dichloromethane (DCM) and mixed together. Before
190 analysis in the GC/MS/MS, the tar/oil product was passed through a packed column of
191 anhydrous sodium sulphate to remove water. Appropriate dilutions of the prepared oil samples
192 were made prior to GC/MS analysis. The DCM extract were then analysed semi-quantitatively
193 on a GC/MS/MS instrument using external standard method. The GC/MS/MS system consisted
194 of a Varian 3800-GC coupled to a Varian Saturn 2200 ion trap MS/MS equipment. The column
195 used was a 30m x 0.25mm inner diameter Varian VF-5ms (DB-5 equivalent), while the carrier
196 gas was helium, at a constant flow rate of 1 ml min⁻¹. The analytical conditions and detection
197 have been detailed elsewhere (Efika et al., 2015). Spectral searches on the installed NIST2008
198 library were used to qualitatively identify the major 'unknown' compounds in the oil products.
199 In addition, FTIR analysis of the raw liquid samples was carried out using a Thermoscientific,

200 Nicolet iS10 spectrometer and the infrared bands recorded was compared with characteristic
201 infrared bands of known organic functional groups in the database. Background correction for
202 the DCM solvent was implemented during FTIR analysis.

203

204 **2.3.3. Analysis of solid residues**

205 After each test, the weight of the solid residue remaining in the sample boat after pyrolysis was
206 determined by subtracting the weight of the sample boat. The surface area of a selection of the
207 recovered solid residues was measured to determine its suitability for further applications e.g.
208 as catalyst supports. The surface area measurement was carried out with the Brunauer, Emmett
209 and Teller (BET) method via nitrogen adsorption in a Quantachrome Corporation (FL, US)
210 Autosorb 1-C instrument. In addition, the HHV of the recovered solid residue was determined
211 using a bomb calorimeter (ASTM, 2000; ASTM D2015).

212

213 **3.0. Results and Discussion**

214 **3.1 Effects of heating rate on Gas, Oil and Solid distribution**

215 Table 2 shows the result of the effect of heating rate on the pyrolysis of waste wood, lignin,
216 cellulose and hemicellulose at a final high temperature of 800 °C. Table 2 shows that three
217 different major product fractions – solid residue, oil/tar and gas - were produced from the tests
218 as expected (Balat, 2008; Bridgwater, 2003; Demirbas, 2001), at a final temperature of 800 °C,
219 and at the chosen average heating rates of 5, 90 and 350 °C min⁻¹. It is clear from Table 2 that
220 varying the heating rate of pyrolysis influenced the yields of the three major products from the
221 four samples. For the wood pellets, gas yields increased from 14.5 wt% at a heating rate of 5
222 °C min⁻¹ to 54.1 wt% at 350 °C min⁻¹, while solid residue yields decreased from 26.7 to 14.2
223 wt%, respectively. The oil/tar yields initially showed an increasing trend from 49.5 to 57.4
224 wt%, with the heating rate, from 5 °C min⁻¹ through to 90 °C min⁻¹. However, when the heating

225 rate was ramped up to $350\text{ }^{\circ}\text{C min}^{-1}$, a sharp reduction in the liquid yield to 27.4 wt% occurred,
226 which corresponded to a sharp increase in the gas yield mentioned earlier (54.1 wt%). Similar
227 results have been obtained from other researchers for the pyrolysis of different biomass
228 feedstocks at high final temperatures of up to $900\text{ }^{\circ}\text{C}$. Williams et al. (Williams & Besler, 1996)
229 reported that increasing the heating rate for pine wood pyrolysis from 5 to $80\text{ }^{\circ}\text{C min}^{-1}$ resulted
230 in increased production of oil and gas while reducing the yield of char. Becidan et al. (Becidan
231 et al., 2007) showed that, compared to the low heating rate, a higher heating rate of $115\text{ }^{\circ}\text{C}$
232 min^{-1} resulted in increased gas yield and reduced liquid and char yield during pyrolysis of waste
233 biomass.

234

235 These results demonstrate how the combination of heating rate and temperature can be very
236 influential for controlling the product yields from pyrolysis. The heating rate in combination
237 with the particle size impacts pyrolysis by affecting how long it takes for the sample to get to
238 the final pyrolysis temperature. More importantly, high heating rates should result in a more
239 even and rapid heat transfer to the loaded sample in the fixed bed reactor, as a result of the
240 relatively small particle size. Therefore, the increased gas yield during investigations at the
241 heating rate of $\approx 350\text{ }^{\circ}\text{C min}^{-1}$, would have resulted from the relatively more uniform
242 degradation of the covalent bonds in the biomass with the activation energy provided by the
243 rapidly increasing temperature. Moreover, the high temperature environment within the reactor
244 heated zone also meant the primary pyrolysis vapours were equally subjected to rapid
245 secondary heating, which led to extensive so called secondary homogenous cracking reactions
246 of the liberated primary pyrolysis products (Blondeau & Jeanmart, 2012), thus converting the
247 biomass derived primary products to the simplest gas molecules. Furthermore, it is expected
248 that although the average heating rate of the bulk sample as measured by the temperature sensor
249 is relatively rapid (6 K s^{-1}), the condition in the reactor was non-isothermal as a result of the

250 particle sizes being $> 300\mu\text{m}$ (Blondeau & Jeanmart, 2011), as well as because of particle being
251 packed into the cylindrical sample holder. This would have created both a temperature and
252 heating rate gradient in the sample, with the particles at the outer layer initially experiencing
253 both much higher heating rate than the bulk average as well as higher temperature than the
254 particles at the centre. These sort of conditions, in addition to encouraging secondary
255 homogenous cracking reactions for primary pyrolysis products, especially from the outer
256 located particles, would have also promoted secondary intra-particle (heterogeneous) cracking
257 reactions of the primary pyrolysis products of the particles located especially in the centre of
258 the cylindrical arrangement (Di Blasi, 2008). This is more so for the most centrally located
259 particles because it is argued that primary pyrolysis products from singular biomass particles
260 would have been released into a somewhat porous wall of other biomass particles hence
261 extending the volatiles-solid contact time as well as cracking effects.

262

263 The quantity of solid residues produced from waste wood pyrolysis declined with the
264 increasing heating rate as shown in Table 2. This is in-line with previous literatures (Ayllón et
265 al., 2006; Williams & Besler, 1996) which reported that low heating rates resulted in more char
266 yield from the pyrolysis of biomass, and vice-versa. The increased char yield impacted by the
267 low heating rate pyrolysis may be explained by the promotion of the cross-linking mechanisms
268 for char formation by extending the time the sample spends at the “optimum char formation
269 temperature region”, (Hoekstra et al., 2012; Weinstetn & Broido, 1970), compared to pyrolysis
270 at higher heating rate.

271 Figure 2 (a to c) shows plots with 2nd order polynomial trendlines, of product yields against
272 heating rate for the different pyrolysed samples and their product fractions (gas, oil and solids)
273 at a fixed final temperature of 800 °C, which shows a similar trends to the work of Di Blasi and
274 co-workers (Di Blasi et al., 1999). This indicated that at the experimental conditions, increasing

275 the heating rate resulted in an intensification of the high temperature effects. The plots also
276 indicated that it was possible to estimate the product yields for pyrolysis at our experimental
277 conditions for our samples using simple 2nd order polynomial equations.

278

279 The products of the separate pyrolysis of lignin, cellulose and hemicellulose exhibited a similar
280 trend to the waste wood sample with increasing heating rate as shown in Table 2. As the heating
281 rate was increased from 5 to 90 °C min⁻¹, the oil and gaseous products increased as a result of
282 the release of volatiles from the solid structure of the samples, while the solid product yield
283 decreased. Cellulose and xylan, behave essentially like the waste wood; at the heating rate of
284 5 °C min⁻¹ oil was the product fraction of the highest yield for the cellulose and xylan while at
285 350 °C, gas production became dominant. On the other hand, lignin produced char as the main
286 product at all heating rates. Pyrolysis of lignin has been reported to produce extensive char due
287 to cross linking reactions from the phenolic fractions (Custodis et al., 2014; Kawamoto, 2017;
288 Patwardhan et al., 2011a).

289 Further examination shows that cellulose yielded the highest oil product (54 wt%) at heating
290 rate of 5 °C min⁻¹, and the highest gaseous product (73.1 wt%) at the heating rate of \approx 350 °C
291 min⁻¹. This is in agreement with the proximate analyses results in Table 1, which shows that
292 cellulose has the highest volatile matter contents of all the three biomass components. Hence,
293 the volatile content was converted mostly into condensable oil/tar during pyrolysis at 5 °C min⁻¹
294 ¹, and mostly into gases during pyrolysis at \approx 350 °C min⁻¹. Compared to the cellulose, the
295 xylan sample produced the higher gas and solids yields at the lower heating rates (5 and 90 °C
296 min⁻¹), while it produced higher solid but lower gas yield at the heating rate of \approx 350 °C min⁻¹.
297 Shen et al. (Shen et al., 2010b) reported more char formation from xylan than cellulose during
298 pyrolysis up to 750 °C, at fast heating rates.

299

300 Table 2 indicates that the increased gas yield noted for the cellulose and xylan samples at the
301 heating rate of $\approx 350 \text{ }^\circ\text{C min}^{-1}$, were as a result of the conversion of the oil products as well as
302 the solid products, especially for cellulose. However, for the lignin sample the increased gas
303 yield was mostly as a result of the cracking of oil products, as the solid residue remained mostly
304 unchanged when the results of lignin pyrolysis at heating rates of $90 \text{ }^\circ\text{C min}^{-1}$ and at $\approx 350 \text{ }^\circ\text{C}$
305 min^{-1} are compared. Caballero et al. (Caballero et al., 1996) pyrolyzed lignin at high heating
306 rate and temperatures up to $900 \text{ }^\circ\text{C}$ and found that the predominant product was char up to 800
307 $^\circ\text{C}$ and then gas followed by char above $800 \text{ }^\circ\text{C}$. Again, considering the low volatile matter
308 content of lignin, the low gas and oil yields was not a surprising result under the investigated
309 conditions in this present study.

310

311 Considering the individual pyrolysis products from the wood, cellulose, xylan and lignin
312 samples, the production of char noted for the wood sample can therefore be linked mostly to
313 its content of lignin and partly from hemicellulose (Burhenne et al., 2013; Shen et al., 2010b).
314 At the same time, the gaseous and oil/tar products from the wood pellet can be linked to the
315 easily degradable volatile contents of mostly its cellulose fraction, with some contributions
316 from the hemicellulose fraction (Burhenne et al., 2013).

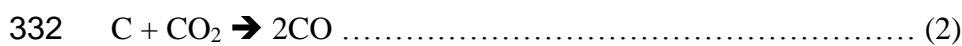
317

318 **3.2 Gas composition**

319 Table 3 shows the detailed compositions and mass yields of components in the gas products
320 from the four samples in relation to heating rate at $800 \text{ }^\circ\text{C}$. Clearly, the yields of the gas
321 components increased with increasing heating rates. The highest gas mass yields were
322 produced at the heating rate of $\approx 350 \text{ }^\circ\text{C min}^{-1}$ due to the promotion of enhanced cracking of
323 the pyrolysis vapours. This is supported by the noted reduction in the quantity of oil/tar
324 obtained from all the samples compared to the lower heating rate experiments. For all four

325 samples , CO was the dominant gas component at the heating rate of 350 °C min⁻¹, and its
326 formation could have resulted from rapid cracking of oxygenated primary volatiles (Duman et
327 al., 2011) and possibly the Boudouard reaction (Radlein, 2002), equation 2. Possible reduced
328 in-situ steam reforming reactions due to the low moisture content of the sample, as well as the
329 presence of hydrogen containing species in the condensed liquid such as aromatics and alkenes,
330 as shown in Table 4 may have contributed to the prevalence of CO in the gaseous product.

331



333

334 For cellulose and xylan, CO formation has been attributed to decarbonylation of carbonyl
335 functional groups in the biomass or the primary degradation products (Li et al., 2001; Shen et
336 al., 2010a; Shen et al., 2010b). The CO₂ and CO products of lignin pyrolysis have been reported
337 to be as a result of the degradation of carbonyl, carboxyl and ether groups while at high
338 temperature CO production is mostly as a result of the cracking of diaryl ether groups (Wang
339 et al., 2009). The high yields of CO from the samples at 350 °C min⁻¹ suggests that the gas
340 products have potential to be further reformed into hydrogen or used for the synthesis of
341 hydrocarbon fuels.

342

343 However, CO₂ was a major gas component in the gas product from all samples at the lower
344 heating rates of 5, 20 and 90 °C min⁻¹. Similar results have been achieved by other researchers
345 (Beaumont & Schwob, 1984; Meesri & Moghtaderi, 2002) for the pyrolysis of wood. The
346 higher yield of CO₂ at these conditions has been explained to be as a result of the primary
347 decomposition of oxygen-containing functional groups, especially the decomposition of
348 carboxylic compounds (Li et al., 2001; Meesri & Moghtaderi, 2002; Shen et al., 2010a; Shen
349 et al., 2010b) due to their highly thermal unstable nature. Some researchers (Yang et al., 2007)

350 compared the pyrolysis of cellulose, xylan and lignin and reported that xylan produced the
351 highest CO₂ content as a result of higher carboxylic content. A comparison of the CO
352 composition for the wood components at $\approx 350\text{ }^{\circ}\text{C min}^{-1}$ heating rate indicates that most of the
353 CO content of wood is likely contributed by cellulosic materials.

354

355 The HHV of the gas produced from the test at this heating rate of $350\text{ }^{\circ}\text{C min}^{-1}$ was also noted
356 to be the highest (18.8 MJ m^{-3}) as shown in Figure 3, compared to the other heating rates. This
357 was as a result of the increased yield of CH₄ and the other hydrocarbon gases C₂ – C₄ in the
358 product gas. For each of the samples, the HHV of the gases from the pyrolysis at $\approx 350\text{ }^{\circ}\text{C min}^{-1}$
359 were the highest due to increased volume of gas produced and higher contents of hydrocarbon
360 gases. Compared to the other wood components, lignin pyrolysis at $\approx 350\text{ }^{\circ}\text{C min}^{-1}$ produced
361 the lowest yield of gases, however the CV of its product gas was the highest among the wood
362 components, due to its high content of hydrocarbons especially methane (Wang et al., 2009;
363 Yang et al., 2007).

364

365 Table 3 shows that during pyrolysis at $\approx 350\text{ }^{\circ}\text{C min}^{-1}$, the cellulose gave the highest wt% of
366 hydrogen but at low heating, lignin produced the highest wt% of hydrogen, which agrees with
367 the work of others (Yang et al., 2007) during the slow pyrolysis of lignin, cellulose and
368 hemicellulose at $900\text{ }^{\circ}\text{C}$. The authors attributed the yield of H₂ to the cracking of C-H aromatic
369 bonds in the lignin and carbonized residues from the other three samples. This resulted from
370 the release of molecular hydrogen during cross-linking polymerization of carbon atoms, which
371 condense into polycyclic aromatic hydrocarbons and then to char.

372

373 **3.3 Semi-quantitative composition of the oil/tar products**

374 Figure 4 shows the spectra from the FTIR analysis of waste wood pyrolysis oil, which indicates
375 the functional group characteristics of the pyrolysis oil from wood slow heating ($5\text{ }^{\circ}\text{C min}^{-1}$)
376 and from fast heating ($\approx 350\text{ }^{\circ}\text{C min}^{-1}$) to $800\text{ }^{\circ}\text{C}$. A comparison of both spectra clearly shows
377 differences in the peak intensities which are representative of the different functional groups
378 present in the liquid products. The spectra demonstrate the differences in the composition of
379 the pyrolysis oils as a result of the different heating rates. The presence of polycyclic,
380 monocyclic and substituted aromatic groups is indicated in the absorption peaks between 675
381 to 900 cm^{-1} and 1572 to 1625 cm^{-1} . The peaks from 950 to 1325 cm^{-1} represent C-O stretching
382 and O-H deformation, indicating the presence of alcohols and phenols (Efika et al., 2015).
383 Peaks between 1350 to 1475 cm^{-1} and 2800 to 3000 cm^{-1} represent C-H deformation and
384 indicates the presence of alkanes or alkyl groups. The presence of alkenes is indicated by the
385 C=C stretching vibrations between peaks 1625 and 1675 cm^{-1} . C=O stretching vibrations are
386 indicated by the peaks between 1650 and 1850 cm^{-1} , while O-H vibrations are indicated by the
387 broad peaks between 3050 and 3600 cm^{-1} , and a combination of these peaks suggests the
388 presence of carboxylic acids and their derivatives.

389

390 Table 4 shows the detected compounds from the GC/MS analysis of the oil products from
391 wood, cellulose, xylan and lignin, and with reference to pyrolysis at the different heating rates
392 investigated. The relative abundance of the detected compounds are indicated by asterisks, so
393 that more asterisks in Table 4 indicates increasing weight percent yields of the identified
394 compound. For simplicity, the compounds in the oil/tar have been classified into oxygenates,
395 phenolics, aliphatic hydrocarbons and aromatic hydrocarbons. Table 4 shows that for the oil
396 product from wood pyrolysis, there was a decrease in oxygenates, while aromatic compounds
397 increased with increasing heating rate. As an indication of the effects of heating rate on the
398 yields of the different classes of organic compounds in the oil/tar, a selection of compounds

399 detected in the oil/tar; representing oxygenates, phenols aliphatic and aromatic hydrocarbons
400 have been made. Figure 5 showed the weight percent yields of cyclopentanone, phenol, indane
401 and naphthalene in the pyrolysis oils from waste wood. Clearly, the yields of naphthalene
402 increased from 0.1 – 3.2 wt%, with increasing heating rate from 5 to ≈ 350 °C min⁻¹ for the
403 pyrolysis of wood. In contrast, the yields of cyclopentanone and phenol showed a decreasing
404 trend. As the heating rate was increased, the high temperature effects were intensified, which
405 resulted in the cracking of products such as the oxygenates and other simple aliphatic
406 compounds, into gases as well into the more thermally stable aromatics via Diels-Alder
407 reactions. Such cyclization and aromatization processes led to increased refining of the oil and
408 loss of sides groups resulting from cleavage of weaker bonds. Such refining reactions at the
409 molecular level would increase aromatic content of the liquid products and also increase the
410 formation in the gas products as seen in Tables 2 and 3.

411
412 The GC/MS results are in agreement with the FTIR spectra presented in Figure 4 which shows
413 an increase in the intensity of the indicative peaks for the monocyclic, polycyclic and
414 substituted aromatic groups, in the spectra for the liquid from pyrolysis at heating rate of 350
415 °C min⁻¹ compared to that at 5 °C min⁻¹. As an illustration, the GC/MS chromatograms of the
416 oils/tars obtained from waste wood pyrolysis at heating rates of 5 °C min⁻¹ and 350 °C min⁻¹
417 have been presented in Supplementary Information File (S11). The chromatograms clearly
418 shows the transition from majority oxygenated and aliphatic compounds at the lower heating
419 rate to a majority lower molecular-weight aromatic hydrocarbons at the higher heating rate.
420 This transition corroborates the FTIR spectra in Figure 4, which shows higher peak intensities
421 for peaks between 1350 to 1475 cm⁻¹, 1625 to 1675 cm⁻¹, 2800 to 3000 cm⁻¹ and between peaks
422 950 to 1325 cm⁻¹, corresponding to the presence of aliphatic compounds (alkanes and
423 oxygenates) in the liquid products, for the pyrolysis at 5 °C min⁻¹ compared to the pyrolysis at

424 350 °C min⁻¹. (Yu et al., 1997) reported an increase in the aromatic content and a decrease in
425 the oxygenate content of oil from wood pyrolysis with increasing temperature from 700 to 900
426 °C. Other researchers (Xianwen et al., 2000) reported that the most abundant hydrocarbons
427 detected from the pyrolysis of wood at 500 °C were alkanes, while (Tsai et al., 2007) reported
428 the presence of many of aromatic compounds as well as oxygenated compounds for the
429 pyrolysis of rice husk to 500 °C, at a heating rate of at 400 °C min⁻¹. The GC/MS
430 chromatograms obtained from the analysis of the liquid products from the biomass model
431 compounds at heating rates of 5 °C min⁻¹ and 350 °C min⁻¹ have been provided in the
432 Supplementary Information [SI1].

433

434 The results of the analysis of the oil products from the pyrolysis of cellulose, xylan and lignin
435 at 5 and \approx 350 °C min⁻¹ are also shown in Table 4, showing similar trends to those obtained
436 from the waste wood sample. For pyrolysis at 5 °C min⁻¹, the most abundant compounds
437 detected for the cellulose, xylan and lignin were oxygenated and aliphatic compounds. The
438 presence of long-chain alkanes (hexadecane and pentadecane) from slow pyrolysis of lignin
439 was reported by (de Wild et al., 2009) during pyrolysis of lignin. The authors reported further
440 increase in the yields of these compounds during the hydro-treatment of the pyrolysis oils, as
441 a result of hydrodeoxygenation reaction of the lignin-derived bio-oil. While during pyrolysis \approx
442 350 °C min⁻¹, the most abundant compounds detected in the oil products from cellulose, xylan
443 and lignin were aromatics. Others have investigated the pyrolysis of lignin to 800 °C, at slow
444 and fast heating rates, and reported increased aromatics at the fast heating conditions while an
445 abundance of oxygenates were detected at the slow heating rate (Windt et al., 2009). Mono-
446 aromatic compounds are also primary decomposition products of lignin (Asmadi et al., 2011),
447 and this explains its relatively higher content in the lignin derived oil at 5 °C min⁻¹. (Shen et
448 al., 2010a) reported an increase in the production of ringed hydrocarbons and a decrease in

449 oxygenates content of the pyrolysis oil with increasing pyrolysis temperature from
450 hemicellulose.

451

452 The pyrolysis of the wood, cellulose, xylan and lignin samples at the heating rate of $\approx 350\text{ }^{\circ}\text{C}$
453 min^{-1} intensified the effect of the high pyrolysis temperature resulting in secondary heating
454 which promoted vapour phase cracking and condensation reactions, leading to the formation
455 of gases and aromatic compounds. However at the heating rate of $5\text{ }^{\circ}\text{C min}^{-1}$, the heating effect
456 was minimized as volatiles were gradually released and swept out of the reactor before its
457 temperature could increase to temperatures at which secondary reactions were encouraged,
458 leading to the formation of mostly oxygenated and aliphatic compounds.

459

460 **3.4 Solid residue characteristics**

461 The BET surface area for the solid residues from wood pyrolysis at the lowest and highest
462 heating rates were measured, and indicated that the solids from the pyrolysis at $5\text{ }^{\circ}\text{C min}^{-1}$, had
463 a higher surface area ($219\text{ m}^2\text{g}^{-1}$) than that for the solids from pyrolysis at $\approx 350\text{ }^{\circ}\text{C min}^{-1}$ (123
464 m^2g^{-1}). This indicated that during pyrolysis at $\approx 350\text{ }^{\circ}\text{C min}^{-1}$, the thermal shock impacted on
465 the wood sample would have caused the volatiles to be violently released from the wood
466 structure, thereby destroying the internal pore structure (Zanzi et al., 1996) of the solid product.
467 In contrast, during pyrolysis at slow heating rate, the volatiles gradually exited the structure of
468 the wood sample. The HHV of the solid residues from both heating rates were similar. For
469 instance, the solid residue obtained at a heating rate of $5\text{ }^{\circ}\text{C min}^{-1}$ had a HHV of 33.9 MJ kg^{-1} ,
470 while at a heating rate of $350\text{ }^{\circ}\text{C min}^{-1}$ it was 33.1 MJ kg^{-1} . Hence, these results demonstrate
471 that high-temperature pyrolysis can be a source of carbonaceous solid materials with large
472 surface areas and coal-like calorific values from biomass.

473

474 **4.0 Conclusions**

475 Overall, this study provided some understanding of high temperature pyrolysis of biomass both
476 as an advanced technology platform for biomass conversion and as pre-processing step for
477 biomass gasification. The pyrolysis of waste wood and its major biochemical components
478 (cellulose, xylan and lignin) were carried out in a fixed bed reactor at three different heating
479 rates and to a final temperature of 800 °C. A combination of heating rate and high temperature
480 gave profound influence on the yields and compositions of solid residue, gas and liquid
481 products as follows, and in no particular order;

482 Firstly, promoted secondary cracking of volatiles and resulted in increased yields of product
483 gases with high calorific values from all four samples. Secondly, Oil/tar products became more
484 aromatic with increasing heating rate from all samples, due to thermal refinement leading to
485 production of highly stable molecules. Finally, Char product with relatively surface areas and
486 coal-like CVs were obtained due to rapid devolatilization of smaller molecules from within
487 particles leading to a char of a highly porous nature.

488

489

490

491

492

493

494

495

496

497

498

499 **5.0 References**

- 500 Asmadi, M., Kawamoto, H., Saka, S. 2011. Gas- and solid/liquid-phase reactions
501 during pyrolysis of softwood and hardwood lignins. *Journal of Analytical and*
502 *Applied Pyrolysis*, **92**(2), 417-425.
- 503 Ayllón, M., Aznar, M., Sánchez, J.L., Gea, G., Arauzo, J. 2006. Influence of
504 temperature and heating rate on the fixed bed pyrolysis of meat and bone meal.
505 *Chemical Engineering Journal*, **121**(2–3), 85-96.
- 506 Balat, M. 2008. Hydrogen-Rich Gas Production from Biomass via Pyrolysis and
507 Gasification Processes and Effects of Catalyst on Hydrogen Yield, Vol. 30,
508 Taylor & Francis, pp. 552 - 564.
- 509 Beaumont, O., Schwob, Y. 1984. Influence of physical and chemical parameters on
510 wood pyrolysis. *Industrial & Engineering Chemistry Process Design and*
511 *Development*, **23**(4), 637-641.
- 512 Becidan, M., Skreiberg, Ø., Hustad, J.E. 2007. Products distribution and gas release
513 in pyrolysis of thermally thick biomass residues samples. *Journal of Analytical*
514 *and Applied Pyrolysis*, **78**(1), 207-213.
- 515 Beis, S.H., Onay, Ö., Koçkar, Ö.M. 2002. Fixed-bed pyrolysis of safflower seed:
516 influence of pyrolysis parameters on product yields and compositions.
517 *Renewable Energy*, **26**(1), 21-32.
- 518 Blondeau, J., Jeanmart, H. 2012. Biomass pyrolysis at high temperatures: Prediction
519 of gaseous species yields from an anisotropic particle. *Biomass and Bioenergy*,
520 **41**(0), 107-121.
- 521 Blondeau, J., Jeanmart, H. 2011. Biomass pyrolysis in pulverized-fuel boilers:
522 Derivation of apparent kinetic parameters for inclusion in CFD codes.
523 *Proceedings of the Combustion Institute*, **33**(2), 1787-1794.
- 524 Bridgwater, A.V. 2003. Renewable fuels and chemicals by thermal processing of
525 biomass. *Chemical Engineering Journal*, **91**(2-3), 87-102.
- 526 Burhenne, L., Messmer, J., Aicher, T., Laborie, M.-P. 2013. The effect of the biomass
527 components lignin, cellulose and hemicellulose on TGA and fixed bed pyrolysis.
528 *Journal of Analytical and Applied Pyrolysis*(0).
- 529 Caballero, J.A., Font, R., Marcilla, A. 1996. Study of the primary pyrolysis of Kraft lignin
530 at high heating rates: yields and kinetics. *Journal of Analytical and Applied*
531 *Pyrolysis*, **36**(2), 159-178.
- 532 Çağlar, A., Demirbas, A. 2002. Hydrogen rich gas mixture from olive husk via
533 pyrolysis. *Energy Conversion and Management*, **43**(1), 109-117.
- 534 Cetin, E., Gupta, R., Moghtaderi, B. 2005. Effect of pyrolysis pressure and heating rate
535 on radiata pine char structure and apparent gasification reactivity. *Fuel*, **84**(10),
536 1328-1334.
- 537 Custodis, V.B.F., Hemberger, P., Ma, Z., van Bokhoven, J.A. 2014. Mechanism of Fast
538 Pyrolysis of Lignin: Studying Model Compounds. *The Journal of Physical*
539 *Chemistry B*, **118**(29), 8524-8531.
- 540 de Wild, P., Van der Laan, R., Kloekhorst, A., Heeres, E. 2009. Lignin valorisation for
541 chemicals and (transportation) fuels via (catalytic) pyrolysis and

- 542 hydrodeoxygenation. *Environmental Progress & Sustainable Energy*, **28**(3),
543 461-469.
- 544 Demirbas, A. 2001. Biomass resource facilities and biomass conversion processing
545 for fuels and chemicals. *Energy Conversion and Management*, **42**(11), 1357-
546 1378.
- 547 Demirbas, A. 2002. Gaseous products from biomass by pyrolysis and gasification:
548 effects of catalyst on hydrogen yield. *Energy Conversion and Management*,
549 **43**(7), 897-909.
- 550 Di Blasi, C. 2008. Modeling chemical and physical processes of wood and biomass
551 pyrolysis. *Progress in Energy and Combustion Science*, **34**(1), 47-90.
- 552 Di Blasi, C., Signorelli, G., Di Russo, C., Rea, G. 1999. Product Distribution from
553 Pyrolysis of Wood and Agricultural Residues. *Industrial & Engineering*
554 *Chemistry Research*, **38**(6), 2216-2224.
- 555 Dufour, A., Girods, P., Masson, E., Rogaume, Y., Zoulalian, A. 2009. Synthesis gas
556 production by biomass pyrolysis: Effect of reactor temperature on product
557 distribution. *International Journal of Hydrogen Energy*, **34**(4), 1726-1734.
- 558 Duman, G., Okutucu, C., Ucar, S., Stahl, R., Yanik, J. 2011. The slow and fast
559 pyrolysis of cherry seed. *Bioresource Technology*, **102**(2), 1869-1878.
- 560 Dupont, C., Commandré, J.-M., Gauthier, P., Boissonnet, G., Salvador, S., Schweich,
561 D. 2008. Biomass pyrolysis experiments in an analytical entrained flow reactor
562 between 1073 K and 1273 K. *Fuel*, **87**(7), 1155-1164.
- 563 Efika, E.C., Onwudili, J.A., Williams, P.T. 2015. Products from the high temperature
564 pyrolysis of RDF at slow and rapid heating rates. *Journal of Analytical and*
565 *Applied Pyrolysis*, **112**(Supplement C), 14-22.
- 566 Elliott, D.C. 2013. Transportation fuels from biomass via fast pyrolysis and
567 hydroprocessing. *Wiley Interdisciplinary Reviews: Energy and Environment*,
568 **2**(5), 525-533.
- 569 Fagbemi, L., Khezami, L., Capart, R. 2001. Pyrolysis products from different
570 biomasses: application to the thermal cracking of tar. *Applied Energy*, **69**(4),
571 293-306.
- 572 Guoxin, H., Hao, H., Yanhong, L. 2009. Hydrogen-Rich Gas Production from Pyrolysis
573 of Biomass in an Autogenerated Steam Atmosphere. *Energy & Fuels*, **23**(3),
574 1748-1753.
- 575 Hoekstra, E., Van Swaaij, W.P.M., Kersten, S.R.A., Hogendoorn, K.J.A. 2012. Fast
576 pyrolysis in a novel wire-mesh reactor: Decomposition of pine wood and model
577 compounds. *Chemical Engineering Journal*, **187**(0), 172-184.
- 578 Kantarelis, E., Donaj, P., Yang, W., Zabaniotou, A. 2009. Sustainable valorization of
579 plastic wastes for energy with environmental safety via High-Temperature
580 Pyrolysis (HTP) and High-Temperature Steam Gasification (HTSG). *Journal of*
581 *Hazardous Materials*, **167**(1-3), 675-684.
- 582 Kawamoto, H. 2017. Lignin pyrolysis reactions. *Journal of Wood Science*, **63**(2), 117-
583 132.
- 584 Lam, C.H., Das, S., Erickson, N.C., Hyzer, C.D., Garedew, M., Anderson, J.E.,
585 Wallington, T.J., Tamor, M.A., Jackson, J.E., Saffron, C.M. 2017. Towards

- 586 sustainable hydrocarbon fuels with biomass fast pyrolysis oil and
587 electrocatalytic upgrading. *Sustainable Energy & Fuels*, **1**(2), 258-266.
- 588 Li, S., Lyons-Hart, J., Banyasz, J., Shafer, K. 2001. Real-time evolved gas analysis by
589 FTIR method: an experimental study of cellulose pyrolysis. *Fuel*, **80**(12), 1809-
590 1817.
- 591 Li, S., Xu, S., Liu, S., Yang, C., Lu, Q. 2004. Fast pyrolysis of biomass in free-fall
592 reactor for hydrogen-rich gas. *Fuel Processing Technology*, **85**(8-10), 1201-
593 1211.
- 594 Luo, Z., Wang, S., Liao, Y., Zhou, J., Gu, Y., Cen, K. 2004. Research on biomass fast
595 pyrolysis for liquid fuel. *Biomass and Bioenergy*, **26**(5), 455-462.
- 596 Mayes, H.B., Broadbelt, L.J. 2012. Unraveling the Reactions that Unravel Cellulose.
597 *The Journal of Physical Chemistry A*, **116**(26), 7098-7106.
- 598 Meesri, C., Moghtaderi, B. 2002. Lack of synergetic effects in the pyrolytic
599 characteristics of woody biomass/coal blends under low and high heating rate
600 regimes. *Biomass and Bioenergy*, **23**(1), 55-66.
- 601 Mettler, M.S., Vlachos, D.G., Dauenhauer, P.J. 2012. Top ten fundamental challenges
602 of biomass pyrolysis for biofuels. *Energy & Environmental Science*, **5**(7), 7797-
603 7809.
- 604 Onay, O., Kockar, O.M. 2003. Slow, fast and flash pyrolysis of rapeseed. *Renewable
605 Energy*, **28**(15), 2417-2433.
- 606 Patwardhan, P.R., Brown, R.C., Shanks, B.H. 2011a. Understanding the Fast
607 Pyrolysis of Lignin. *ChemSusChem*, **4**(11), 1629-1636.
- 608 Patwardhan, P.R., Dalluge, D.L., Shanks, B.H., Brown, R.C. 2011b. Distinguishing
609 primary and secondary reactions of cellulose pyrolysis. *Bioresource
610 Technology*, **102**(8), 5265-5269.
- 611 Radlein, D. 2002. Study of Levoglucosan. in: *Fast Pyrolysis of Biomass: A Handbook*,
612 (Eds.) A.V. Bridgwater, S. Czernik, J. Diebold, D. Meier, A. Oasmaa, C.
613 Peacocke, J. Piskorz, D. Radlein, Vol. 2, CPL Press. Newbury, UK, pp. 165.
- 614 Seebauer, V., Petek, J., Staudinger, G. 1997. Effects of particle size, heating rate and
615 pressure on measurement of pyrolysis kinetics by thermogravimetric analysis.
616 *Fuel*, **76**(13), 1277-1282.
- 617 Shen, D.K., Gu, S., Bridgwater, A.V. 2010a. Study on the pyrolytic behaviour of xylan-
618 based hemicellulose using TG-FTIR and Py-GC-FTIR. *Journal of Analytical
619 and Applied Pyrolysis*, **87**(2), 199-206.
- 620 Shen, D.K., Gu, S., Bridgwater, A.V. 2010b. The thermal performance of the
621 polysaccharides extracted from hardwood: Cellulose and hemicellulose.
622 *Carbohydrate Polymers*, **82**(1), 39-45.
- 623 Sun, S., Tian, H., Zhao, Y., Sun, R., Zhou, H. 2010. Experimental and numerical study
624 of biomass flash pyrolysis in an entrained flow reactor. *Bioresource
625 Technology*, **101**(10), 3678-3684.
- 626 Tsai, W.T., Lee, M.K., Chang, Y.M. 2007. Fast pyrolysis of rice husk: Product yields
627 and compositions. *Bioresource Technology*, **98**(1), 22-28.

- 628 Wang, G., Li, W., Li, B., Chen, H. 2008. TG study on pyrolysis of biomass and its three
629 components under syngas. *Fuel*, **87**(4-5), 552-558.
- 630 Wang, S., Wang, K., Liu, Q., Gu, Y., Luo, Z., Cen, K., Fransson, T. 2009. Comparison
631 of the pyrolysis behavior of lignins from different tree species. *Biotechnology
632 Advances*, **27**(5), 562-567.
- 633 Wei, L., Xu, S., Zhang, L., Zhang, H., Liu, C., Zhu, H., Liu, S. 2006. Characteristics of
634 fast pyrolysis of biomass in a free fall reactor. *Fuel Processing Technology*,
635 **87**(10), 863-871.
- 636 Weinstetn, M., Broido, A. 1970. Pyrolysis-Crystallinity Relationships in Cellulose.
637 *Combustion Science and Technology*, **1**(4), 287-292.
- 638 Williams, P.T. 2005. *Waste Treatment and Disposal. 2nd Edition ed.* John Wiley &
639 Sons, Ltd.
- 640 Williams, P.T., Besler, S. 1996. The influence of temperature and heating rate on the
641 slow pyrolysis of biomass. *Renewable Energy*, **7**(3), 233-250.
- 642 Windt, M., Meier, D., Marsman, J.H., Heeres, H.J., de Koning, S. 2009. Micro-pyrolysis
643 of technical lignins in a new modular rig and product analysis by GC–MS/FID
644 and GC x GC–TOFMS/FID. *Journal of Analytical and Applied Pyrolysis*, **85**(1–
645 2), 38-46.
- 646 Xianwen, D., Chuangzhi, W., Haibin, L., Yong, C. 2000. The Fast Pyrolysis of Biomass
647 in CFB Reactor. *Energy & Fuels*, **14**(3), 552-557.
- 648 Yang, H., Yan, R., Chen, H., Lee, D.H., Zheng, C. 2007. Characteristics of
649 hemicellulose, cellulose and lignin pyrolysis. *Fuel*, **86**(12–13), 1781-1788.
- 650 Yu, Q., Brage, C., Chen, G., Sjöström, K. 1997. Temperature impact on the formation
651 of tar from biomass pyrolysis in a free-fall reactor. *Journal of Analytical and
652 Applied Pyrolysis*, **40–41**(0), 481-489.
- 653 Zanzi, R., Sjöström, K., Björnbom, E. 1996. Rapid high-temperature pyrolysis of
654 biomass in a free-fall reactor. *Fuel*, **75**(5), 545-550.
- 655 Zanzi, R., Sjöström, K., Björnbom, E. 2002. Rapid pyrolysis of agricultural residues at
656 high temperature. *Biomass and Bioenergy*, **23**(5), 357-366.
- 657 Zhang, J., Nolte, M.W., Shanks, B.H. 2014. Investigation of Primary Reactions and
658 Secondary Effects from the Pyrolysis of Different Celluloses. *ACS Sustainable
659 Chemistry & Engineering*, **2**(12), 2820-2830.
660
- 661
- 662
- 663
- 664
- 665
- 666

667

668

669

670 **List of Figures**

671

672 Figure 1: Schematic of the reactor system

673

674 Figure 2: Yields from the pyrolysis of wood and components to 800 °C and at different heating
675 rates: (a) Gas yields, (b) Solid yields (c) Oil yields;

676

677 Figure 3: Higher heating values of the gas products obtained from high temperature pyrolysis
678 of waste wood and biomass components in relation to heating rates

679

680 Figure 4: FTIR spectrograms for the oil/tar products obtained from high temperature pyrolysis
681 of waste wood and biomass components in relation to heating rates

682

683 Figure 5: Actual yields of selected compounds in the oil/tar obtained from high temperature
684 pyrolysis of waste wood and biomass components in relation to heating rates

685

686

687 **Nomenclature**

688 min Minute

689 wt% Weight percentage

690 vol% Volume percentage

691 CV Calorific value

692 μm Micro metre

693 GC Gas chromatography
 694 MS Mass spectroscopy
 695 TCD Thermal conductivity detector
 696 FID Flame ionization detector
 697 HHV higher heating value
 698 Z_m Gas compressibility factor
 699 FTIR Fourier transforms infra-red
 700 DCM Dicloromethane
 701 BET Brunauer, Emmett and Teller
 702 K Kelvin temperature
 703 s Second
 704 \approx Approximately
 705

706

707 List of Tables

708

709 Table 1: Proximate and Ultimate compositions of waste wood sample and biomass
 710 model compounds used in this work

	Waste wood	Cellulose	Xylan	Lignin
Ultimate analysis (wt%)				
C	46.6	41.7	40.3	61.3
H	5.8	5.9	5.5	5.1
N	0.40	0.41	0.41	1.1
S	nd	nd	nd	0.7
O (by diff, ash free)	38.2	52	49.8	27.7
Proximate analysis (wt%)				
Moisture	7.0	5.0	6.0	4.0
Ash	2.0	-	4.0	4.0
Volatile Matter	76	82	73	56
Fixed carbon	15	13	17	36

711 nd: not detected

712

713
714

Heating rates	5 °C min ⁻¹				90 °C min ⁻¹				≈ 3	
Results wt% of sample	wood	cellulose	xylan	lignin	wood	cellulose	xylan	lignin	wood	cellu
Gas	14.5	21.0	27.1	16.4	17.5	21.3	27.3	16.5	52.9	73.1
solid	26.7	16.0	27.2	43.7	20.8	12.4	22.9	37.6	15.7	5.9
Oil	49.5	54.0	36.9	35.9	57.4	65.4	42.9	40.6	27.5	16.7
Mass Balance	90.8	91.0	91.2	96.0	95.7	99.0	93.0	94.7	96.1	95.6

715
716
717
718
719
720
721
722
723
724
725
726
727
728
729
730
731
732
733
734
735
736

Table 2: Product yields and mass balances from the high temperature pyrolysis of waste wood and biomass components in relation to heating rates

737

738

739

740 Table 3: Compositional yields of gas products (in wt% and volume %) from high
 741 temperature pyrolysis of waste wood and biomass components in relation to heating
 742 rates (nitrogen-free)

Heating rates	5 °C min ⁻¹				90 °C min ⁻¹				≈ 350 °C min ⁻¹			
	wood	cellulose	xylan	lignin	wood	cellulose	xylan	lignin	wood	cellulose	xylan	lignin
Yields, wt% of sample												
H ₂	0.4	0.4	0.6	1.0	0.4	0.3	0.6	0.7	0.8	1.4	1.0	0.8
CO	5.6	6.3	7.1	6.1	6.3	6.7	9.0	6.9	30.3	44.5	16.8	15.9
CO ₂	7.2	13.0	17.5	6.2	9.2	13.1	16.0	5.8	10.9	14.7	20.3	5.7
CH ₄	1.0	0.8	0.7	2.6	1.2	0.7	0.8	2.6	4.8	5.0	2.7	4.4
C ₂ - C ₄	0.3	0.6	1.2	0.5	0.4	0.5	0.9	0.5	6.1	7.3	3.7	2.4
Yields, volume % sample												
H ₂	32.7	25.7	30.3	47.7	24.8	21.3	27.8	38.8	18.1	22.0	26.3	28.4
CO	31.0	28.4	24.4	21.4	33.3	31.5	30.6	27.1	48.7	50.2	32.9	39.0
CO ₂	25.5	37.6	38.0	13.7	28.8	39.3	34.6	14.5	11.2	10.6	25.4	9.0
CH ₄	9.6	6.6	4.4	16.0	11.2	6.0	4.5	18.2	13.6	9.9	9.1	18.9
C ₂ H ₄	0.4	0.4	0.4	0.2	0.6	0.5	0.4	0.3	5.7	4.7	3.9	2.5
C ₂ H ₆	0.5	0.5	1.4	0.5	0.7	0.6	1.2	0.6	0.8	1.3	1.2	0.8
C ₃ H ₆	0.2	0.3	0.3	0.1	0.3	0.5	0.3	0.1	1.1	0.8	0.6	0.6
C ₃ H ₈	0.1	nd	0.3	0.1	0.1	0.0	0.4	0.4	0.2	0.1	0.2	0.2
C ₄ H ₈ & C ₄ H ₆	nd	0.4	0.2	0.1	0.1	0.1	0.1	0.0	0.6	0.2	0.4	0.6
C ₄ H ₁₀	nd	0.2	0.4	0.2	0.0	0.1	0.1	0.0	0.0	0.3	0.0	0.0
Gross Calorific values (MJ/kg)												
	8.1	9.2	13.4	13.0	8.0	8.0	12.7	11.3	24.1	35.8	25.4	16.7

nd: not detected

743

744

745

746 Table 4: List and indicative concentrations of different classes of compounds
 747 detected from GC/MS analysis of oil/tar products derived from high temperature
 748 pyrolysis of waste wood and biomass components in relation to heating rates

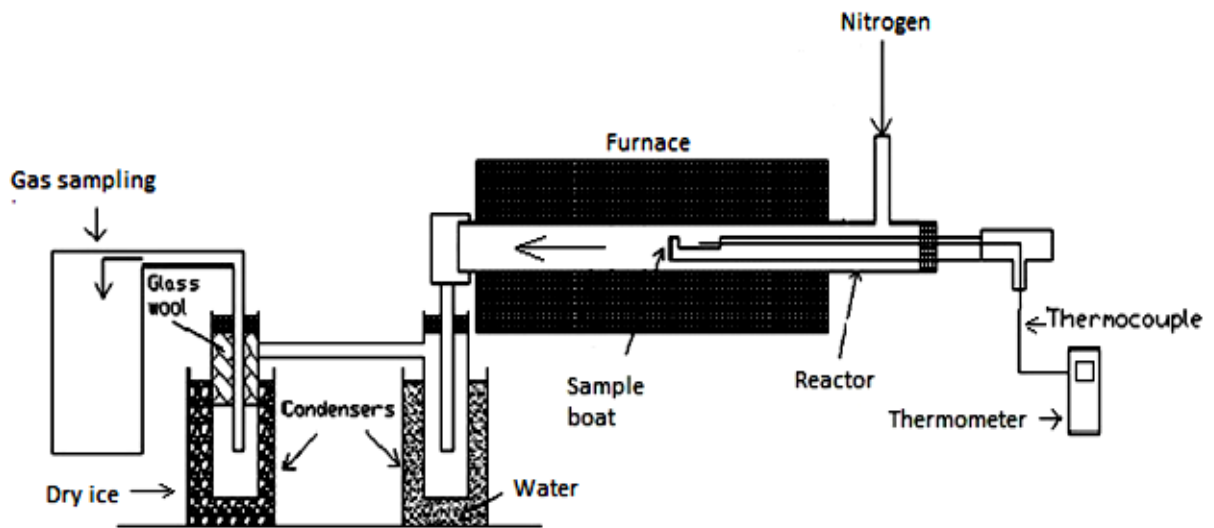
Heating rate	5 °C min ⁻¹				≈ 350 °C min ⁻¹	
	wood	cellulose	xylan	lignin	wood	cellulose
Identified compounds	Oxygenates					
Cyclopentanone	***	****	****	****	**	*
Furfural						
Anisole	*	*	**	**		
Phenol	***				*	
Acetophenone		***	****	**		
	Phenolics					
2,4-Dimethylphenol			****			
1,2-Benzenediol						
2,3,5-Trimethylphenol	**	****			***	
4-Isopropylphenol	****	**				
Dibenzofuran		****		*		
	Aromatic hydrocarbons					
Styrene	*	*				****
o-Xylene	*	*				
Alphamethylstyrene	***		*		**	*
Betamethylstyrene	*		*	*	***	***
Indane	*	*	**	*	***	*
Indene	*	*	*	*	***	***
1,2,3,4-Tetramethylbenze						
Naphthalene	*	**	**	*	****	****
2-Methylnaphthalene			**	*		****
1-Methylnaphthalene		***	**			
Biphenyl	***	*	*	*	*	****
2-Ethyl-naphthalene				*		
1-Ethyl-naphthalene						***
2,6-Dimethylnaphthalene	*	*	*	***		
1,4-Dimethylnaphthalene	**	*	**	***	***	
Fluorene	***	*	*	*		
1,3-Diphenylpropane						
Phenanthrene		*		*		
1-Phenylnaphthalene	**					
o-Terphenyl		**				
Fluoranthene		*			*	
Pyrene	*		*		**	
m-Terphenyl			*			
1,3,5-Triphenylbenzene	***		**	*	***	**
	Alkanes					
Octane, C8		***	***	***		*
Decane, C10	***	**	**	**	*	
Undecane, C11	**	***	***	***	*	*

Dodecane, C12	***	***	***	*	*
Tridecane, C13	**			*	*
Tetradecane, C14			***		
Pentadecane, C15				***	
Hexadecane, C16			*		
Phytane			*	*	*
Heptadecane, C17			*	*	
Pristane			***		*
Octadecane, C18				*	
Eicosane, C20					
Alkenes					
Octene, C8		**			
Nonene, C9					***
Decene, C10		****		***	
Undecene, C11			***		
Dodecene, C12				***	
Tridecene, C13				*	
Tetradecene, C14					
Pentadecene, C15					***

749

750 List of Figures

751



752

753

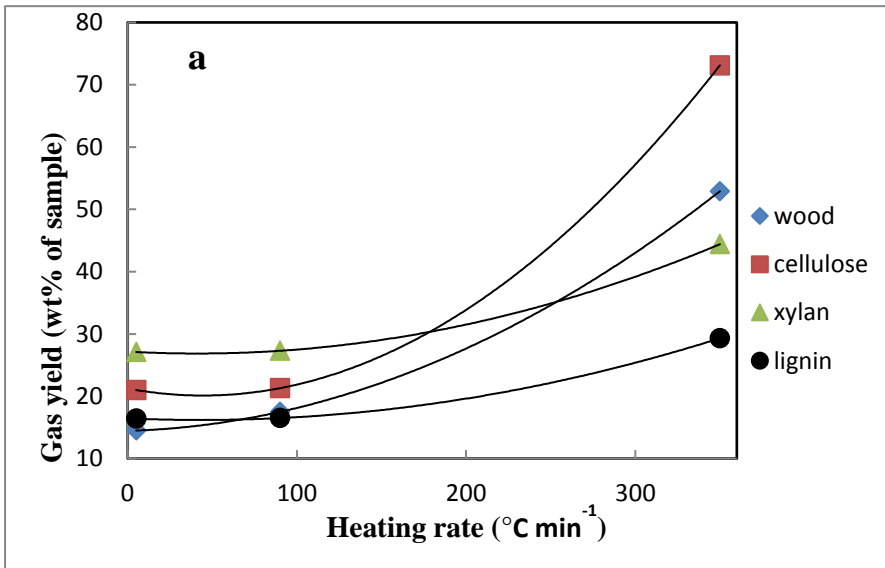
754 Figure 1

755

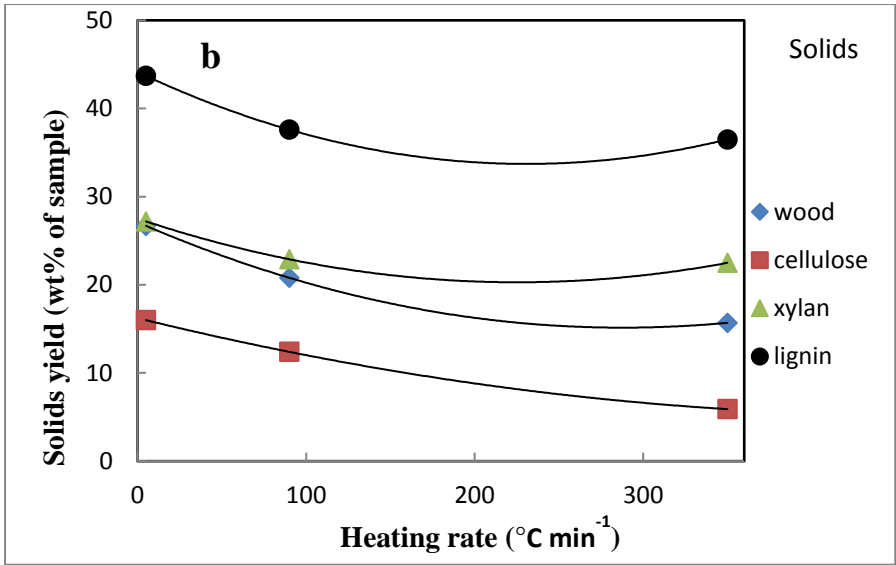
756

757

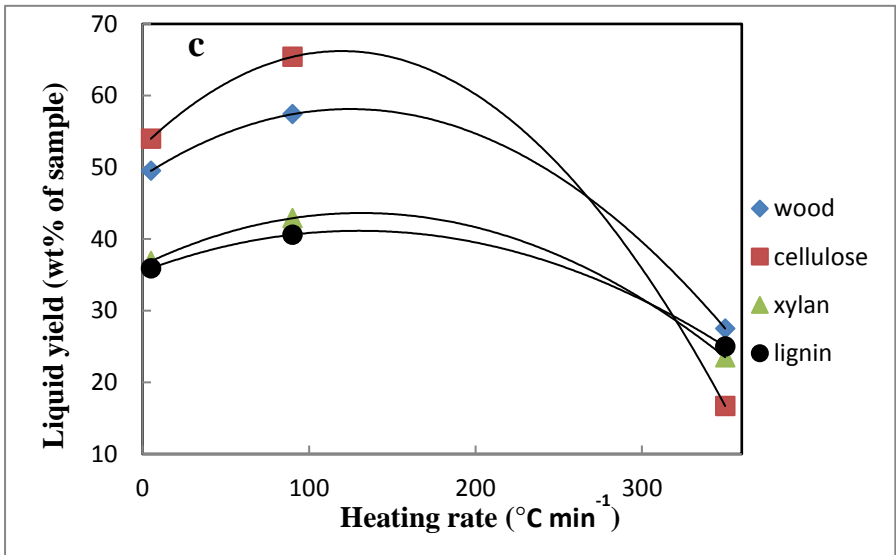
758
759
760
761
762
763
764
765
766
767
768
769
770
771
772



773



774



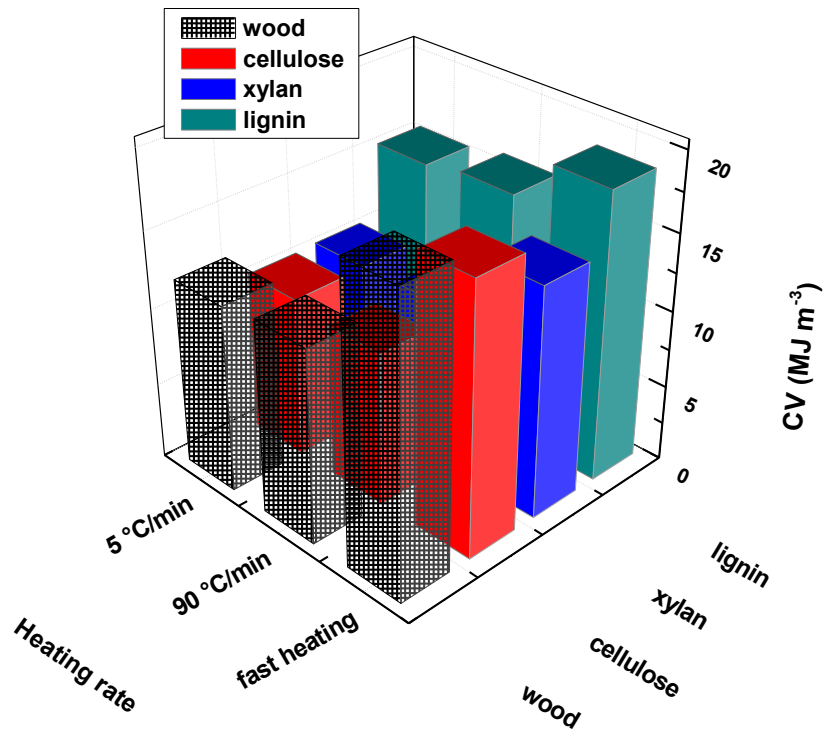
775

776 Figure 2

777

778

779



780

781 Figure 3

782

783

784

785

786

787

788

789

790

791

792

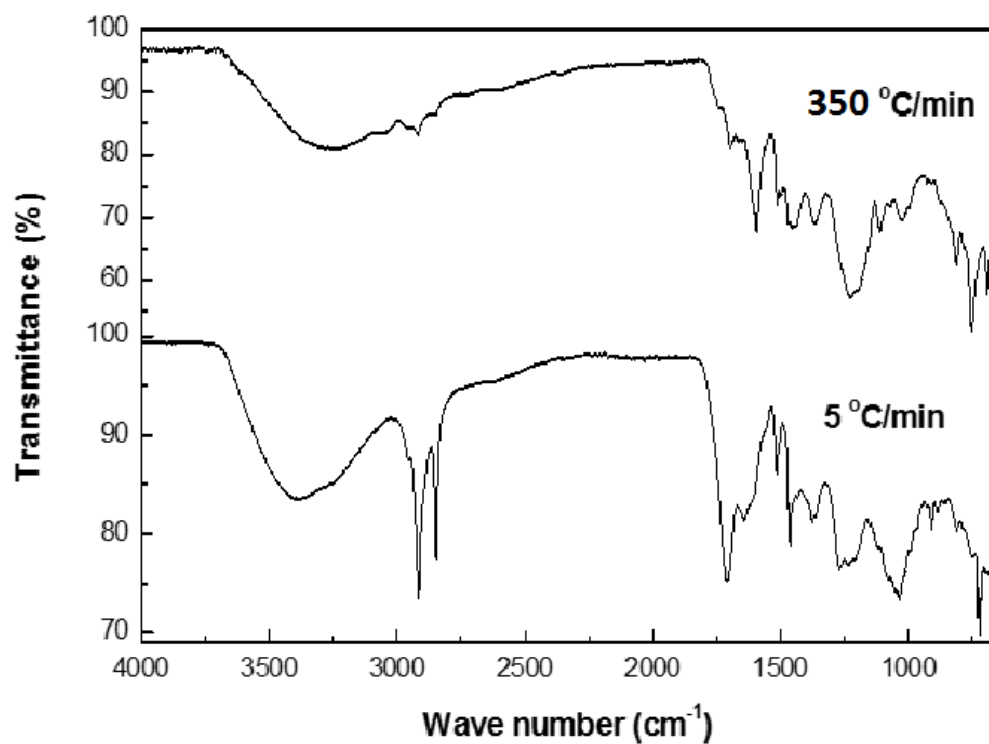
793

794

795

796

797



798

799 Figure 4

800

801

802

803

804

805

806

807

808

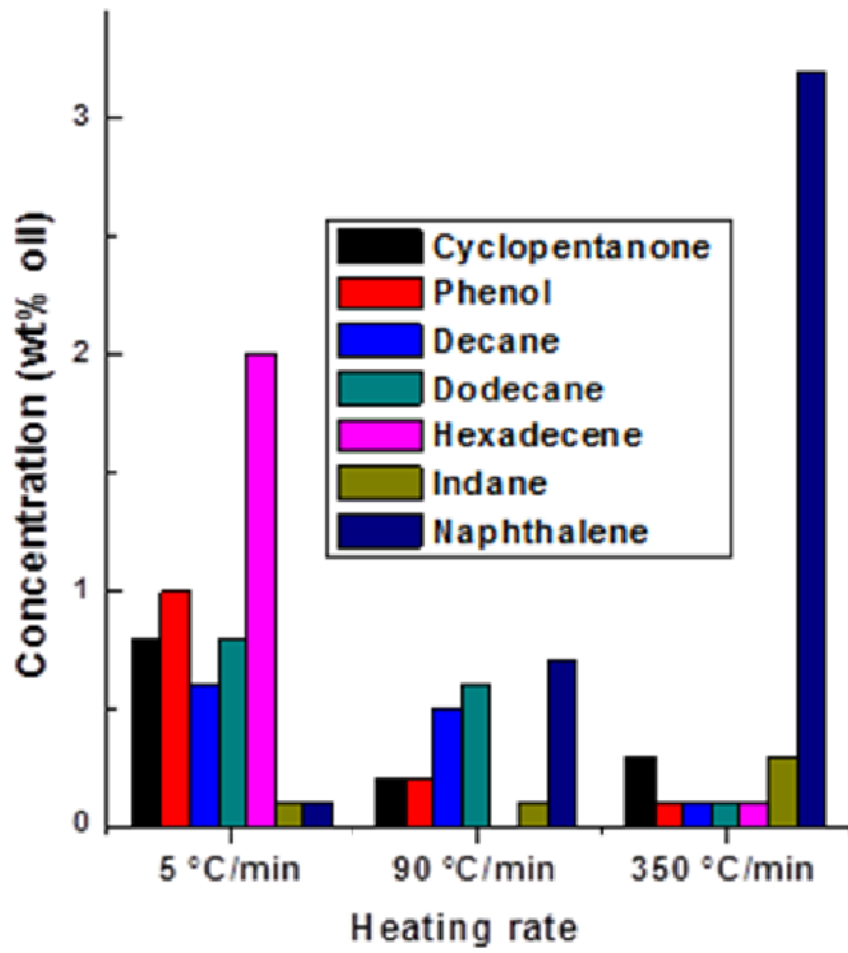
809

810

811

812

813



814
 815 Figure 5
 816
 817
 818
 819
 820
 821
 822
 823
 824
 825